

N.V. Ivanova · V.M. Pugatchev · V.A. Nevostruev  
N.A. Kolpakova

## Phase analysis of platinum-mercury and platinum-lead electrolytic deposits

Received: 13 September 2001 / Accepted: 24 February 2002 / Published online: 11 April 2002  
© Springer-Verlag 2002

**Abstract** By means of X-ray diffraction, the phase composition of electrolytic deposits obtained during simultaneous electrodeposition of platinum with lead, and of platinum with mercury, on glassy carbon was investigated. Formation of dispersed platinum ( $D \approx 65\text{--}110 \text{ \AA}$ ) in both binary system cases, of a solid solution of platinum-lead and of the intermetallic compound  $\text{PtHg}_4$  was proved. During the anodic scan up to a potential of  $+0.75 \text{ V}$  in  $0.1 \text{ M HCl}$ , the compound  $\text{PtHg}_4$  undergoes partial oxidation; electrolytic platinum is resistant to oxidation under these conditions.

**Keywords** X-ray diffraction · Electrodeposition · Platinum · Lead · Mercury

### Introduction

Previous investigations have proved that an oxidation peak of metallic platinum is not observed in the range of the working potentials of stripping voltammetry under any conditions [1, 2]. Using a neutron activation technique, noticeable electrooxidation of compact platinum has been shown only in the range of potentials not less than  $+1.2 \text{ V}$  (vs.  $\text{Ag/AgCl}$ ) in  $0.1\text{--}1 \text{ M HCl}$ , and proved that the process occurs with the formation of chlorides of platinum [3, 4]. However, the simultaneous electrodeposition of platinum and one of four electrochemically active metals (mercury, copper, lead or cadmium) on the surface of a glassy carbon or graphite electrode

resulted in the appearance on the anodic voltammogram of an additional electropositive current peak, depending on the concentration of  $\text{PtCl}_6^{2-}$  (or  $\text{PtCl}_4^{2-}$ ) (Figs. 1 and 2). The increase of the additional current peak is accompanied by decrease of the current peak for oxidation of the metal. At a definite concentration ratio of the binary system components, the magnitude of the current of the additional peak becomes constant, and the current oxidation peak of the electronegative metal disappears. The proportional relationship of the additional peak current with the concentration of the platinum ions makes possible an anodic stripping analysis of platinum in the presence of mercury, copper, lead or cadmium [1, 2, 5]. However, in order to find out the mechanism of the co-electrodeposition and the anodic oxidation of the binary systems of platinum with one of these elements (including the nature of the additional anodic current peak), the structure of the obtained metallic deposits needs detailed analysis under conditions of the voltammetric experiment. In this study, by means of X-ray diffraction the phase composition of binary electrodeposits of platinum-mercury and platinum-lead was investigated.

### Experimental

Voltammetric experiments were performed with a PU-1 (Russia) polarograph in a three-electrode cell consisting of the working glassy carbon electrode (with a geometric surface area of  $0.28 \text{ cm}^2$ ), a reference  $\text{Ag/AgCl}$  ( $3 \text{ M KCl}$ ) electrode, and a Pt wire auxiliary electrode. The working electrode was polished in an  $\text{Al}_2\text{O}_3$  slurry. All potentials are reported relative to the  $\text{Ag/AgCl}$  ( $3 \text{ M KCl}$ ) reference electrode. All solutions were prepared with triply distilled water and ultrapure grade reagents.

The components of the binary systems were electrodeposited from  $0.1 \text{ M HCl}$  or  $0.1 \text{ M HNO}_3$  solutions with various ratios of the concentrations of  $\text{PtCl}_6^{2-}$  and metal (Pb or Hg) at the potential of the diffusion current of the metal (for  $\text{Hg}^{2+}$ ,  $E = -0.7 \text{ V}$ ; for  $\text{Pb}^{2+}$ ,  $E = -1.2 \text{ V}$ ). Then the electrooxidation during the anodic scan was carried out.

Electrodeposition of the samples was performed under conditions of voltammetric experiments; the concentrations of the binary system components ranged from  $8 \times 10^{-4}$  to  $4 \times 10^{-3} \text{ M}$ . For X-ray

N.V. Ivanova (✉) · V.M. Pugatchev · V.A. Nevostruev  
Department of Analytical Chemistry,  
Kemerovo State University, Krasnaya 6,  
Kemerovo 650043, Russia  
E-mail: vbor@mail.kuzbass.net  
Tel.: +7-3842-230605

N.A. Kolpakova  
Department of Physical and Analytical Chemistry,  
Tomsk Technical University,  
Lenina 30, Tomsk 634034, Russia

diffraction analysis the deposit was removed from the electrode surface and placed into the glass sample holder. X-ray diffraction analysis was performed with DRON-3 (Russia) diffractometer with

copper filtered radiation. Tabulated values of the interplanar spacings were taken from X-ray diffraction data cards [6].

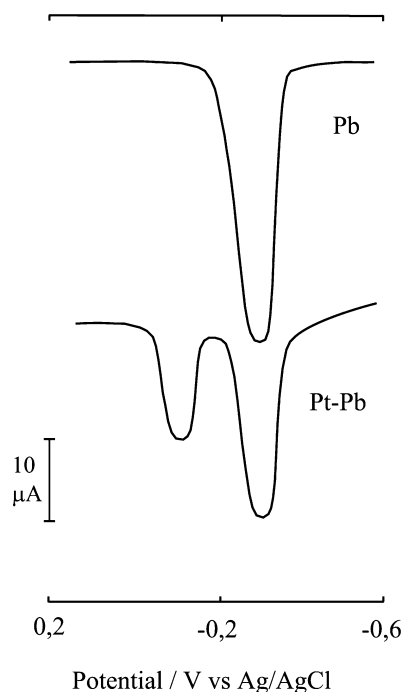


**Fig. 1.** Anodic voltammograms for pure lead and the platinum-lead binary system. Deposition solution:  $7 \times 10^{-5}$  M  $\text{Pb}(\text{NO}_3)_2 + 2 \times 10^{-5}$  M  $\text{PtCl}_6^{2-} + 0.1$  M HCl

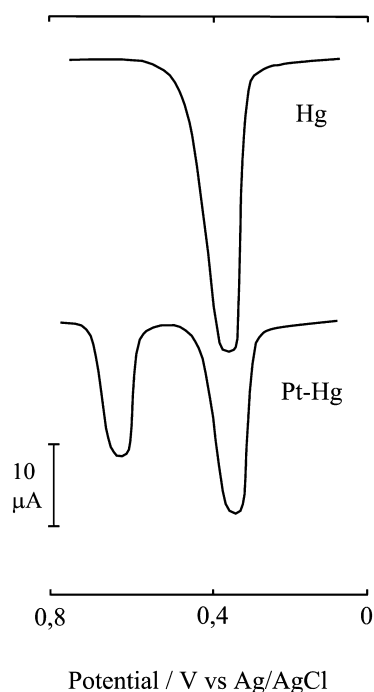


**Fig. 2.** Anodic voltammograms for pure mercury and the platinum-mercury binary system. Deposition solution:  $0.1$  M  $\text{HNO}_3 + 5 \times 10^{-5}$  M  $\text{Hg}(\text{NO}_3)_2$  and then  $0.1$  M HCl +  $1 \times 10^{-5}$  M  $\text{PtCl}_6^{2-}$

## Results and discussion

### Platinum-lead

In the case of the Pt-Pb electrolytic samples, the X-ray pattern showed the diffraction peaks of the cubic lattice of platinum. Reflections of metallic platinum are characterized by a considerable half-width, and the value of the half-width remains approximately identical for all peaks (Fig. 3, Table 1). Therefore it is possible to conclude that the widening is the consequence of a high degree of dispersity of platinum in the electrodeposits. By using the value of the half-width of the diffraction peak on the X-ray pattern, the average value for the size of the platinum particles ( $D$ ) in accordance with the Scherer equation [7] was estimated as:

$$D = \frac{0.9\lambda}{\beta \cos \Theta} \quad (1)$$

where  $\lambda$  is the wavelength ( $\text{\AA}$ ),  $\beta$  is the half-width (rad) and  $\Theta$  is the Bragg angle (rad). For the molar ratios Pt/Pb =  $1/4$  and  $1/30$  in the deposition solution,  $D$  was equal to  $65 \pm 15$   $\text{\AA}$  and  $100 \pm 25$   $\text{\AA}$ , respectively.

For the ratio Pt/Pb =  $1/4$  the diffraction peaks of the platinum lattice were asymmetrical: the half-width in the range of smaller angles was larger than the one in the range of greater angles (Fig. 3). By increasing the lead amount, this asymmetry increased. In the case of the ratio  $1/30$ , the diffraction peaks are shifted to a range of smaller angles in comparison with the diffraction peaks of pure platinum (Table 1b). These facts may be explained by an increase of the parameters of the platinum lattice because of the formation of a solid solution of lead in platinum during the electrodeposition.

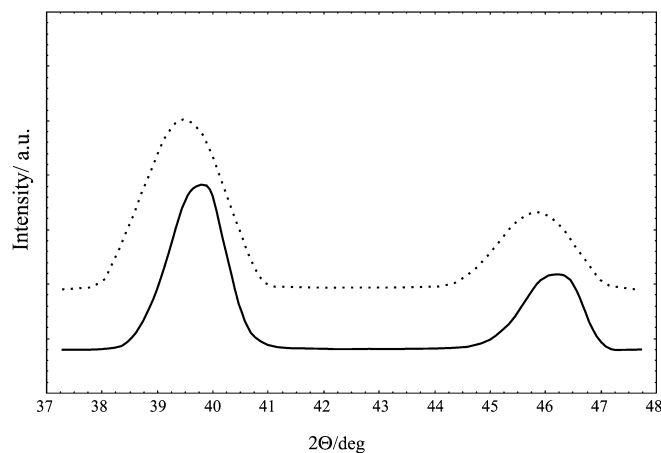


**Fig. 3.** X-ray pattern of the platinum-lead electrolytic sample: Pt/Pb ratio  $1/3$  (full line); Pt/Pb ratio  $1/30$  (dotted line)

**Table 1.** Interplanar spacings for the diffraction peaks of the platinum-lead electrolytic sample in comparison with the tabulated values

(a) Relative intensities for Pt/Pb = 1/3		<i>hkl</i>	<i>d</i> <sub>tab</sub> (Pt) (Å)	<i>d</i> <sub>exp</sub> (Pt) (Å)
Tabulated	Experimental			
100	100	111	2.265	2.266
53	52	200	1.962	1.962
31	30	220	1.387	1.388
(b) Relative intensities for Pt/Pb = 1/30		<i>hkl</i>	<i>d</i> <sub>tab</sub> (Pt <sub>5-7</sub> Pb) (Å)	<i>d</i> <sub>exp</sub> (Å)
Tabulated	Experimental			
100	100	111	2.342	2.287
60	53	200	2.020	1.982
60	31	220	1.431	1.407

It is a matter of common observation that the increase of the interplanar spacings may be used for the estimation of mean mole fractions of the components in the solid solution. However, a relationship of the interplanar spacings of the Pb mole fraction ( $x_{\text{Pb}}$ ) for this binary system has apparently not been described. According to the phase diagram, in the range of small  $x_{\text{Pb}}$  the compound Pt<sub>3</sub>Pb (cubic,  $a = 4.052$ ) exists [8]; other authors [6, 8] report the composition Pt<sub>5-7</sub>Pb for this phase. The experimental values of the lattice constants lay between the constants for the platinum lattice and the constants for the lattice Pt<sub>3</sub>Pb (Pt<sub>5-7</sub>Pb) (Table 1). On the assumption of a linear increase of the lattice constants from Pt (cubic) to Pt<sub>3</sub>Pb or Pt<sub>5-7</sub>Pb (cubic), we estimated the mean value of  $x_{\text{Pb}}$  in the electrodeposited phase, using lattice constants for the compounds Pt<sub>3</sub>Pb (Pt<sub>5-7</sub>Pb) and our experimental data. The  $x_{\text{Pb}}$  value obtained ranges from 0.04 to 0.08. However, if we take into consideration the existence of the compound Pt<sub>3</sub>Pb only, then a  $x_{\text{Pb}}$  value between 0.06 and 0.08 is obtained.

The formation of solid solution of lead in platinum may cause the appearance of an additional anodic peak on the voltammetric curve.

It is necessary to note that on the X-ray pattern the signals for pure lead were not present up to the ratio Pt/Pb = 1/30, although, according to the voltammetric data, the formation of pure lead had occurred on the electrode surface under the same conditions (Fig. 1). When the electrodeposition of lead only was performed from solutions of 0.1 M HCl + 2 × 10<sup>-3</sup> M Pb(NO<sub>3</sub>)<sub>2</sub>, reflexes of the cubic lattice of lead were observed on the X-ray pattern (Table 2).

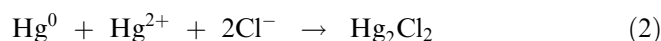
The disappearance of the metallic lead signals may be explained by screening of the lead phase on the electrode surface by metallic platinum. This process may occur if the co-electrodeposition of the components is accom-

panied by reduction of a more electropositive metal on the surface of a more electronegative one. Such a phenomenon may be explained as follows: the electrodeposition of dispersed platinum is accompanied by catalytic electroreduction of H<sub>3</sub>O<sup>+</sup> ions [9, 10, 13, 14] and by partial screening of the platinum surface by gaseous hydrogen. The metallic lead inhibits this process [10] and, therefore, the preferential deposition of platinum on the lead surface occurs.

The metallic platinum has considerable absorption capacity (the mass absorption coefficient under these conditions is 205 cm<sup>2</sup>/g) and, consequently, at a thickness of the platinum layer on lead of 1 μm, for example, only 4% of the initial intensity of the diffraction peaks of lead will be observable on the X-ray pattern.

#### Platinum-mercury

The electrodeposition of mercury from a solution of 0.1 M HCl + 2 × 10<sup>-3</sup> M Hg(NO<sub>3</sub>)<sub>3</sub> both in the presence and absence of PtCl<sub>6</sub><sup>2-</sup> at a potential of -0.7 V resulted in the formation of insoluble calomel on the electrode surface. X-ray data for these samples are shown in Table 3. Calomel is formed by the following reaction [11, 12]:



To avoid the effect of Cl<sup>-</sup> on mercury film formation, the electrodeposition of mercury was performed from a separate solution of 0.1 M HNO<sub>3</sub> + 2 × 10<sup>-3</sup> M Hg(NO<sub>3</sub>)<sub>3</sub>; then the electrode was immediately rinsed and transferred to a 0.1 M HCl + 1 × 10<sup>-3</sup> M PtCl<sub>6</sub><sup>2-</sup> solution.

Under these conditions, the electrodeposition of platinum and mercury on the electrode surface resulted

**Table 2.** Interplanar spacings and relative intensities for the diffraction peaks of electrolytic lead in comparison with the tabulated values

Relative intensities		<i>hkl</i>	<i>d</i> <sub>tab</sub> (Pb) (Å)	<i>d</i> <sub>exp</sub> (Å)
Tabulated	Experimental			
100	100	111	2.855	2.856
50	50	200	2.475	2.475
31	32	220	1.750	1.751

**Table 3.** Interplanar spacings and relative intensities for the diffraction peaks of electrolytically deposited calomel

Relative intensities		<i>d</i> <sub>tab</sub> (Hg <sub>2</sub> Cl <sub>2</sub> ) (Å)	<i>d</i> <sub>exp</sub> (Hg <sub>2</sub> Cl <sub>2</sub> ) (Å)
Tabulated	Experimental		
100	100	3.16	3.16
97	95	4.14	4.14
53	54	2.06	2.06
47	47	1.96	1.96
38	40	1.97	1.97

**Table 4.** Interplanar spacings and relative intensities for the diffraction peaks of the platinum-mercury electrolytic sample

Relative intensities		$hkl$	$d_{\text{tab}}(\text{PtHg}_4)$ (Å)	$d_{\text{exp}}(\text{PtHg}_4)$ (Å)
Tabulated	Experimental			
100	100	220	2.190	2.191
75	30	422	1.267	1.266
70	40	200	3.095	3.099
50	18	420	1.385	1.387
25	14	211	2.510	2.509
Relative intensities		$hkl$	$d_{\text{tab}}(\text{Pt})$ (Å)	$d_{\text{exp}}(\text{Pt})$ (Å)
100	100	111	2.265	2.267
53	53	200	1.962	1.963

in the formation of an intermetallic compound with the composition  $\text{PtHg}_4$  (body-centered cubic lattice) (Fig. 4, Table 4). According to the phase diagram of this binary system, other intermetallic compounds of the composition  $\text{PtHg}_2$  and  $\text{PtHg}$  may exist [6, 8]. The main reflection for  $\text{PtHg}_2$  [(111),  $I/I_0=100\%$ ] is at the same position as the  $\text{PtHg}_4$  (220) diffraction peak, but the other reflections of the  $\text{PtHg}_2$  phase [(200),  $I/I_0=80\%$ ; (311),  $I/I_0=80\%$ ; (100),  $I/I_0=50\%$ ] were not observed on the X-ray pattern. The  $\text{PtHg}_4$  experimental peak intensities are not in accordance with the tabulated ones: the diffraction peaks for (200), (211), (420) and (422) are characterized by smaller intensities (Table 4). It may be the consequence of a contribution of the  $\text{PtHg}_2$  main reflection in the  $\text{PtHg}_4$  (220) reflection. Thus, there is some probability of the formation of a small amount of  $\text{PtHg}_2$  during the electrodeposition.

Apart from the signals for the intermetallide, diffraction peaks for dispersed platinum ( $D \approx 80$  Å) were observed on the X-ray pattern (Fig. 4).

In order to determine the electrochemical stability or instability of the intermetallic compound  $\text{PtHg}_4$  during the anodic scan, the oxidation of the electrolytic deposit was performed in the range of potentials of the additional current peak on the voltammogram (+0.7 to +0.75 V). In this case, the X-ray pattern shows peaks of dispersed

platinum only (Fig. 4). That is, platinum is not oxidized under these conditions but the intermetallic compound  $\text{PtHg}_4$  is decomposed. Either the electrooxidation of mercury from the intermetallic compound or the electrooxidation of both components of the compound may cause this decomposition, which results in the appearance of the additional current peak on the anodic stripping curve. Considering the constancy of the area under both stripping peaks at a constant quantity of mercury [2, 5], it is reasonable to conclude that the additional peak describes the ionization process of mercury from the intermetallic compound with platinum.

The processes of the anodic oxidation of the platinum-lead and platinum-mercury electrolytic deposits were concluded to be similar because of the identical electrochemical behavior [2, 5] of both binary systems. Hence, the electrodeposition of a metal (lead or mercury) in the presence of platinum results in the distribution of this metal between the different phases on the electrode surface: a phase of the pure metal and a phase of the solid solution (or intermetallic compound) with platinum. Electronegative components of the binary phases are capable of electrochemical ionization without platinum oxidation during the anodic scan. Therefore, the process of oxidation of a metal from the different phases leads to the formation of the stripping peaks of the same metal at the different potentials.

**Acknowledgements** The authors thank Dr. Yury Ivanov and Dr. Anatoly Mokhov for helpful discussions.

## References

1. Kolpakova NA, Nemova VV (1974) *Electrokhimiya* 4:1772
2. Dominova IG, Kolpakova NA, Stromberg AG (1977) *J Anal Khim* 10:1980
3. Tchomodanov AN, Kolotyркиn YM, Kosmatiy VE, Dembrovskiy MA (1968) *Electrokhimiya* 12:1466
4. Tchomodanov AN, Kolotyркиn YM, Dembrovskiy MA (1970) *Electrokhimiya* 4: 460
5. Kolpakova NA, Borisova NV, Nevsrtuev VA (2001) *J Anal Khim* 8: 835
6. ASTM (1977) X-ray diffraction data cards. American Society for Testing and Materials, Philadelphia
7. Umanskiy YS (1960) *Rentgenografiya metallov*. Metallurgisdat, Moscow

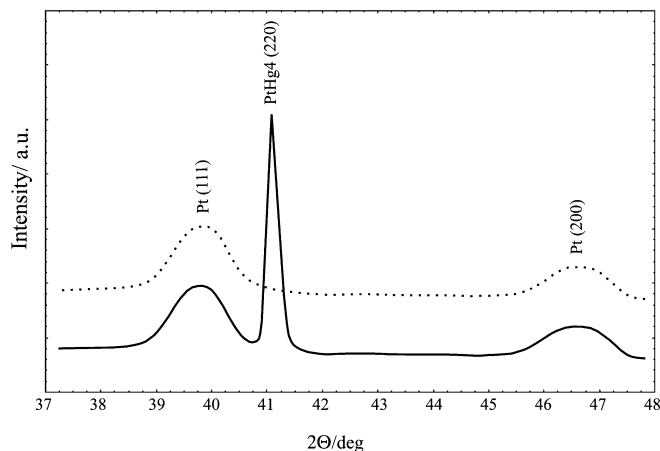


**Fig. 4.** X-ray pattern of the platinum-mercury electrolytic sample before (full line) and after (dotted line) the anodic scan

8. Hansen M, Anderko K (1958) Constitution of binary alloys. McGraw-Hill, New York
9. Bagotzky VS, Vassiljev YB, Hazova OA (1971) Electrochim Acta 17:100
10. Frumkin AN (1987) In: Nikolskiy BP (ed) Elektroodnye processy. Nauka, Moscow
11. Jagner D, Sahlin E, Renman L (1996) Anal Chem 68:1616
12. Jagner D (1978) Anal Chem 50:1924
13. Slendyk J, Herasymenko P (1932) Z Phys Chem 162:223
14. Slendyk J (1932) Collect Czech Chem Commun 4:335